Targeting gene-modified hematopoietic cells to the central nervous system: Use of green fluorescent protein uncovers microglial engraftment

Josef Priller[1], Alexander Flügel[2], Tim Wehner[1], Matthias Boentert[1], Carola A. Haas[3], Marco Prinz[4], Francisco Fernández-Klett[1], Konstantin Prass[1], Ingo Bechmann[5], Bauke A. de Boer[6], Michael Frotscher[3], Georg W. Kreutzberg[2], Derek A. Persons[7] & Ulrich Dirnagl[1]

[1]*Department of Neurology, Charité, Humboldt-University, Berlin, Germany*
[2]*Max-Planck-Institute of Neurobiology and Klinikum Grosshadern, Munich, Germany*
[3]*Institute of Anatomy, University of Freiburg, Freiburg, Germany*
[4]*Max Delbrück Center for Molecular Medicine, Berlin-Buch, Germany*
[5]*Department of Anatomy, Charité, Humboldt-University, Berlin, Germany*
[6]*DRFZ, 10117 Berlin, Germany*
[7]*Department of Hematology and Oncology, St. Jude Children's Research Hospital, Memphis, Tennessee, USA*
Correspondence should be addressed to J.P.; email: josef.priller@charite.de

Gene therapy in the central nervous system (CNS) is hindered by the presence of the blood–brain barrier, which restricts access of serum constituents and peripheral cells to the brain parenchyma. Expression of exogenously administered genes in the CNS has been achieved *in vivo* using highly invasive routes, or *ex vivo* relying on the direct implantation of genetically modified cells into the brain. Here we provide evidence for a novel, noninvasive approach for targeting potential therapeutic factors to the CNS. Genetically-modified hematopoietic cells enter the CNS and differentiate into microglia after bone-marrow transplantation. Up to a quarter of the regional microglial population is donor-derived by four months after transplantation. Microglial engraftment is enhanced by neuropathology, and gene-modified myeloid cells are specifically attracted to the sites of neuronal damage. Thus, microglia may serve as vehicles for gene delivery to the nervous system.

Microglia are the resident immunological effector cells of the central nervous system (CNS). They are activated in response to minor pathological changes in the CNS, and they have a key role in the defense of the neural parenchyma against infection, inflammation, ischemia, trauma, brain tumors and neurodegeneration[1]. Recently, cells derived from bone marrow (BM) were found to enter the brain in adult life to differentiate into microglia, astrocytes and neurons[2–4]. Here we have used transplantation of gene-marked BM cells to characterize the spatiotemporal kinetics of CNS microglial engraftment. In addition, we have evaluated the potential of gene-modified hematopoietic cells to mobilize from the blood and to differentiate into microglia at sites of CNS damage. In three separate lesion models for stroke (focal cerebral ischemia), cholinergic fiber degeneration (fimbria–fornix transection or ff-t) and motoneuron injury (facial-nerve axotomy), genetically modified hematopoietic cells were found to engraft in the CNS and differentiate into microglia at the sites of neuronal injury. Microglial differentiation occured even in the absence of blood–brain barrier disruption, underscoring the utility of gene-engineered hematopoietic cells for gene therapy of the CNS.

Retroviral transfer of *GFP* into murine hematopoietic cells

Donor BM cells were genetically modified with a murine stem-cell virus (MSCV)-based retroviral vector (Fig. 1*a*) encoding the enhanced green fluorescent protein (GFP)[5]. The MSCV vector provides stable long-term gene expression in murine hematopoietic stem cells and blood elements of all lineages[5,6]. By virtue of a mutation within the primer-binding site and lack of one of two direct repeat elements, MSCV is less susceptible to gene silencing *in vivo* compared to other retroviral vectors.

BM cells transduced with the GFP vector were transplanted into lethally irradiated adult C57BL/6 mice. After four weeks, GFP-marked peripheral-blood-cell progeny were analyzed (Fig. 1*b*). We found efficient gene transfer into repopulating hematopoietic cells as demonstrated by the large proportions of peripheral-blood lymphocyte and myeloid cells expressing GFP (approximately 60%). For comparison, when BM cells from transgenic mice that ubiquitously express GFP (ref. 7) were transplanted, on average 75% of peripheral-blood mononuclear cells expressed the fluorophore (data not shown). GFP-expression was stable over the entire observation period of 15 wk after BM transplant (Fig. 1*b*), suggesting that no significant gene silencing occured *in vivo*. There was no evidence of graft-versus-host disease in the transplanted animals (data not shown).

Table 1 Microglial engraftment in the lesioned CNS

Lesion model	Evaluated area	Control side		Lesion side	
		GFP⁺cells	% ramified	GFP⁺ cells	% ramified
Ischemia	Hemisphere	68 ± 9	5	3815 ± 2098*	28
Fimbria-fornix transection	Septal complex	24 ± 3	57	400 ± 109**	27
Facial nerve axotomy	Facial nucleus	5 ± 2	0	18 ± 2**	28

Number of GFP-expressing cells and percentage of ramified cells in the lesioned versus control brain areas 14 d after transient focal cerebral ischemia, 12 d after fimbria-fornix transection and 14 d after facial nerve axotomy in mice transplanted with GFP-transduced BM cells (expressed as mean ± s.e.m.; $n = 6$). An unpaired Student's *t*-test was performed for statistical evaluation of the data. *, $P < 0.05$; **, $P < 0.005$.

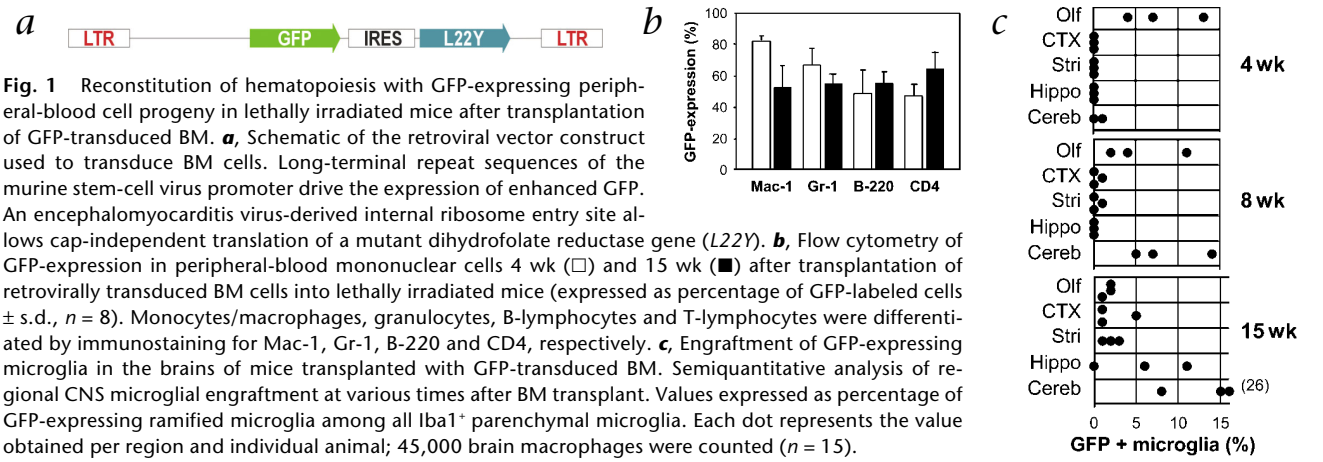

Fig. 1 Reconstitution of hematopoiesis with GFP-expressing peripheral-blood cell progeny in lethally irradiated mice after transplantation of GFP-transduced BM. ***a***, Schematic of the retroviral vector construct used to transduce BM cells. Long-terminal repeat sequences of the murine stem-cell virus promoter drive the expression of enhanced GFP. An encephalomyocarditis virus-derived internal ribosome entry site allows cap-independent translation of a mutant dihydrofolate reductase gene (*L22Y*). ***b***, Flow cytometry of GFP-expression in peripheral-blood mononuclear cells 4 wk (□) and 15 wk (■) after transplantation of retrovirally transduced BM cells into lethally irradiated mice (expressed as percentage of GFP-labeled cells ± s.d., $n = 8$). Monocytes/macrophages, granulocytes, B-lymphocytes and T-lymphocytes were differentiated by immunostaining for Mac-1, Gr-1, B-220 and CD4, respectively. ***c***, Engraftment of GFP-expressing microglia in the brains of mice transplanted with GFP-transduced BM. Semiquantitative analysis of regional CNS microglial engraftment at various times after BM transplant. Values expressed as percentage of GFP-expressing ramified microglia among all Iba1$^+$ parenchymal microglia. Each dot represents the value obtained per region and individual animal; 45,000 brain macrophages were counted ($n = 15$).

Gene-marked hematopoietic cells differentiate into microglia

In the brains of BM chimeric mice, GFP-expressing cells were detected in perivascular and leptomeningeal sites as early as two weeks after BM transplant (data not shown). None of these cells displayed the ramified morphology characteristic of microglia. However, at four wk post-transplant, ramified GFP-transduced cells appeared in the brain parenchyma of the olfactory bulb and cerebellum (Fig. 2*a*). The number of GFP-expressing ramified cells increased significantly in the brain by 15 wk after transplantation (Fig. 2*b* and 1*c*). GFP-positive ramified cells were also detected in BM chimeras from transgenic mice that ubiquitously express GFP (Fig. 2*c*). The engrafted cells strongly expressed the marker gene as determined by direct fluorescence microscopy (Fig. 2*a–c*), as well as by im-

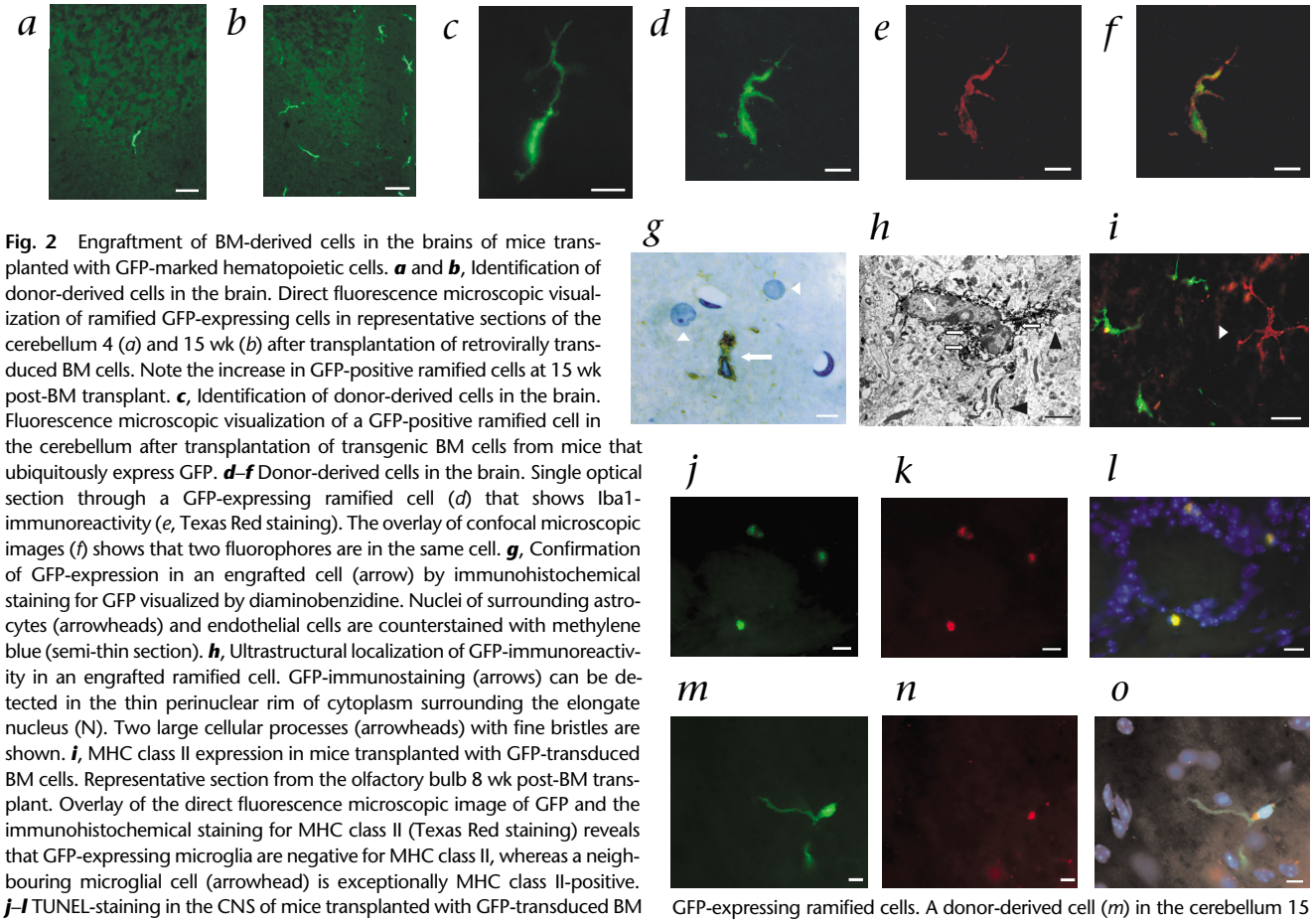

Fig. 2 Engraftment of BM-derived cells in the brains of mice transplanted with GFP-marked hematopoietic cells. ***a*** and ***b***, Identification of donor-derived cells in the brain. Direct fluorescence microscopic visualization of ramified GFP-expressing cells in representative sections of the cerebellum 4 (*a*) and 15 wk (*b*) after transplantation of retrovirally transduced BM cells. Note the increase in GFP-positive ramified cells at 15 wk post-BM transplant. ***c***, Identification of donor-derived cells in the brain. Fluorescence microscopic visualization of a GFP-positive ramified cell in the cerebellum after transplantation of transgenic BM cells from mice that ubiquitously express GFP. ***d–f*** Donor-derived cells in the brain. Single optical section through a GFP-expressing ramified cell (*d*) that shows Iba1-immunoreactivity (*e*, Texas Red staining). The overlay of confocal microscopic images (*f*) shows that two fluorophores are in the same cell. ***g***, Confirmation of GFP-expression in an engrafted cell (arrow) by immunohistochemical staining for GFP visualized by diaminobenzidine. Nuclei of surrounding astrocytes (arrowheads) and endothelial cells are counterstained with methylene blue (semi-thin section). ***h***, Ultrastructural localization of GFP-immunoreactivity in an engrafted ramified cell. GFP-immunostaining (arrows) can be detected in the thin perinuclear rim of cytoplasm surrounding the elongate nucleus (N). Two large cellular processes (arrowheads) with fine bristles are shown. ***i***, MHC class II expression in mice transplanted with GFP-transduced BM cells. Representative section from the olfactory bulb 8 wk post-BM transplant. Overlay of the direct fluorescence microscopic image of GFP and the immunohistochemical staining for MHC class II (Texas Red staining) reveals that GFP-expressing microglia are negative for MHC class II, whereas a neighbouring microglial cell (arrowhead) is exceptionally MHC class II-positive. ***j–l*** TUNEL-staining in the CNS of mice transplanted with GFP-transduced BM cells. At 8 wk after BM transplant, GFP-labeled bodies (*j*) that are TUNEL-stained (*k*) can be found in a representative section of the olfactory bulb. Overlay of the images and counterstaining of nuclei with Hoechst (blue; *l*) demonstrates that the GFP-fragments are apoptotic bodies incorporated into phagocytic cells. No nuclei are TUNEL-stained. ***m–o***, Phagocytic capacity of GFP-expressing ramified cells. A donor-derived cell (*m*) in the cerebellum 15 wk post-BM transplant contains two TUNEL-stained bodies (*n*). Overlay of the images and counterstaining of nuclei with Hoechst (*o*) indicates that the apoptotic bodies are not themselves GFP-positive, but are incorporated into an engrafted GFP-expressing cell. Scale bars: 40 µm (*a* and *b*); 10 µm (*c–f* and *j–l*); 5 µm (*g* and *m–o*); 1 µm (*h*); 20 µm (*i*).

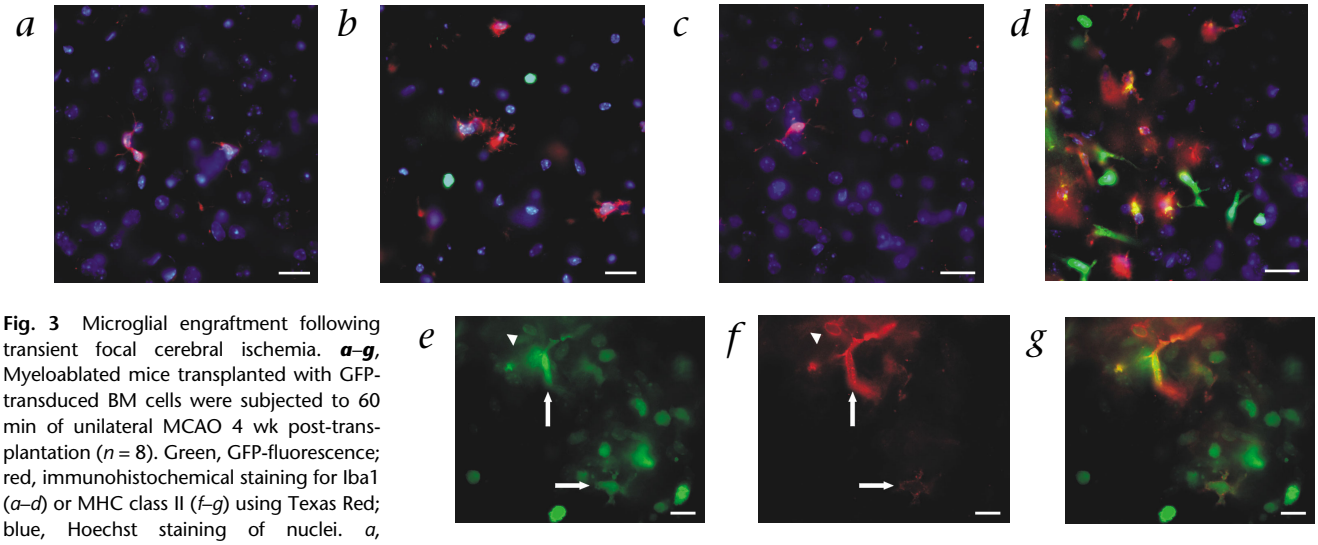

Fig. 3 Microglial engraftment following transient focal cerebral ischemia. ***a–g***, Myeloablated mice transplanted with GFP-transduced BM cells were subjected to 60 min of unilateral MCAO 4 wk post-transplantation ($n = 8$). Green, GFP-fluorescence; red, immunohistochemical staining for Iba1 (*a–d*) or MHC class II (*f–g*) using Texas Red; blue, Hoechst staining of nuclei. *a*, Representative section of the non-ischemic contralateral cortex 24 h after MCAO. *b*, Representative section of the ischemic cortex 24 h after MCAO. *c*, Representative section of the non-ischemic contralateral cortex 14 d after MCAO. *d*, Representative section of the ischemic cortex 14 d after MCAO. *e–g*, A GFP-marked perivascular cell (upper arrow) and a ramified microglial cell (lower arrow) in the ischemic cortex 14 d after MCAO (*e*) express MHC class II (*f*). Only one GFP-positive round cell (*e*, arrowhead) is also MHC class II-positive (*f*, arrowhead). The overlay of images (*g*) shows that GFP is localized in the cytoplasm, whereas MHC class II is expressed on the cell surface. Scale bars: 20 μm (*a–d*); 10 μm (*e–g*).

munohistochemistry using an antibody against GFP (Fig. 2*g*). Ultrastructural analysis revealed the elongate nucleus with heterochromatin and the thin perinuclear rim of cytoplasm characteristic of microglial cells. Immunoelectron microscopic localization of GFP showed a homogenous cytoplasmic distribution (Fig. 2*h*), suggesting that the cell fluorescence resulted from true expression of the marker gene in transduced donor marrow-derived cells, rather than from phagocytosis of GFP-cellular debris by host resident phagocytes. The ramified GFP-marked cells that had engrafted in the CNS were found to express monocyte/macrophage-specific antigens, such as F4/80 and Iba1 (ref. 8) (Fig. 2*d–f*). Moreover, these cells were negative for major histocompatibility complex (MHC) class I and II (Fig. 2*i*), and $CD45^{Lo}$ as determined by FACS analysis (J.P. *et al.* unpublished data), providing further evidence for their microglial identity[9]. By 15 wk after BM transplantation, donor-derived microglial cells were detected in all regions of the brain. At this time, up to 26% of the cerebellar microglia were of hematopoietic origin (Fig. 1*c*). The nuclei of GFP-expressing microglia were never TUNEL-stained, but GFP-positive apoptotic bodies could be found in the brain parenchyma, particularly in the olfactory bulb (Fig. 2*j–l*). On rare occasions TUNEL-stained bodies were detected within ramified GFP-expressing cells (Fig. 2*m–o*), suggesting that the rate of host cell apoptosis was unaltered.

Enhanced microglial engraftment following CNS injury

In order to investigate whether the generation of microglia from hematopoietic cells is enhanced during CNS pathology, we tested monocyte/macrophage engraftment following transient focal cerebral ischemia in GFP-chimeras four wk after BM transplant. At this time, no donor-derived microglia are detectable in the cortex, striatum and hippocampus of chimeric mice (Fig. 1*c*). However, 24 hours after transient middle cerebral artery occlusion (MCAO), a massive infiltration of GFP-labeled round-shaped cells confined to the ischemic cortex, striatum and hippocampus was observed (Fig. 3*a* and *b*). After 14 d, donor BM-derived cells that had infiltrated the lesioned parenchyma differentiated into Iba1-positive microglia (Fig. 3*d* and Table 1). Most of these cells expressed MHC class II (Fig. 3*e–g*). The unaffected contralateral hemisphere was virtually devoid of GFP-expressing cells (Fig. 3*c* and Table 1).

CNS microglial engraftment was also evaluated in a more selective lesion model: transection of the fimbria-fornix results in retrograde changes of septohippocampal projection neurons located in the medial septum, and in anterograde degeneration of cholinergic hippocamposeptal fibers in the lateral septum[10]. When unilateral ff-t was performed in GFP-chimeras 10 wk after BM transplant, GFP-expressing cells selectively infiltrated the lesioned septum and hippocampus, and preferentially located in the lateral septum containing the degenerating terminals of hippocamposeptal fibers (Fig. 4*a*). Three d after lesioning, GFP-labeled round-shaped cells were found to exit the vasculature in the lateral septum (Fig. 4*b*). The projection neurons of the medial septum were still expressing choline acetyltransferase (Fig. 4*b*). After 12 d, ipsilateral loss of acetylcholinesterase staining in the hippocampus indicated retrograde reaction of cholinergic neurons, and completeness of the ff-t (Fig. 4*c*). By this time, the GFP-expressing cells that had infiltrated the lesioned septum acquired a ramified morphology reminiscent of microglia (Fig. 4*d* and Table 1). Very few GFP-positive cells were detected in the unaffected contralateral septal complex (Fig. 4*c* and Table 1).

Finally, GFP-chimeras were subjected to unilateral facial nerve axotomy. In this experimental paradigm, the blood–brain barrier is left intact and remote lesion of the CNS leads to local microglial activation in the CNS (ref. 1). After 14 d, ramified GFP-expressing cells were found to ensheath the axotomized motoneurons in the facial nucleus (Fig. 4*f* and Table 1). These cells were identified as microglia by their expression of the Iba1 antigen (Fig. 4*h–j*). The unlesioned contralateral facial nucleus was devoid of GFP-expressing microglia (Fig. 4*g* and Table 1).

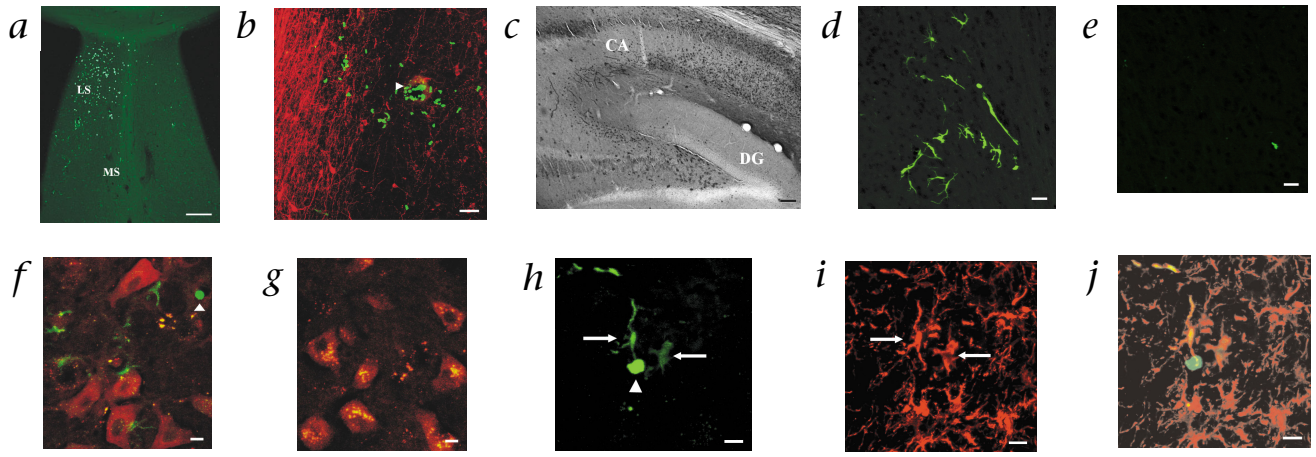

Fig. 4 Microglial engraftment following ff-t and facial nerve axotomy. Lethally irradiated mice transplanted with GFP-transduced BM cells were subjected to ff-t ($n = 11$) or facial nerve axotomy ($n = 9$) 10 and 14 wk post-BM transplant, respectively. ***a***, Confocal laser scanning microscopy of GFP-expressing cells in a representative section of the septal complex 3 wk after unilateral ff-t. GFP-marked cells preferentially infiltrate the deafferented lateral septum (LS) compared to the medial septum (MS). The contralateral unlesioned septal complex is almost devoid of GFP-expressing cells. ***b***, Perivascular infiltration (arrowhead) of GFP-expressing leukocytes in the septum 3d after ff-t. Overlay of GFP-fluorescence and choline acetyltransferase staining. ***c***, Loss of fiber staining for acetylcholinesterase in the hippocampus after ff-t. Note the pronounced loss of staining in the dentate gyrus (DG). Single acetylcholinesterase-positive fibers are visible in the hippocampal subfields (CA). ***d*** and ***e***, Microglial differentiation of BM-derived cells in the lesioned septal complex 12 d after unilateral ff-t. Confocal laser scanning microscopy of a representative section reveals ramified GFP-marked cells in the deafferented septum (*d*), while the unlesioned contralateral septum is devoid of GFP-expressing microglia (*e*). ***f*** and ***g***, Microglial differentiation of BM-derived cells in the facial nucleus 14 d after axotomy. The cell bodies of the damaged motoneurons (*red*; immunohistochemistry for choline acetyltransferase visualized using Cy3) are covered by ramified GFP-expressing microglia (*f*). An infiltrating GFP-labeled lymphocyte (immunohistochemical identification not shown) is indicated by an arrowhead. No GFP-expressing cells are visible in the facial nucleus of the unoperated side of the same representative section (*g*). ***h–j*** Ramified GFP-expressing cells in the facial nucleus 14 d after axotomy (*h*, arrows) express the Iba1 antigen (*i*, immunostaining visualized using Cy3). The overlay (*j*) demonstrates that the two fluorophores are in the same cell (single optical sections using confocal microscopy). A GFP-expressing lymphocyte (*h*, arrowhead; immunohistochemical identification not shown) is Iba1-negative (*i* and *j*). Scale bars: 100 μm (*a*); 50 μm (*b* and *c*); 20 μm (*d, e*); 10 μm (*f–j*).

Discussion

This study demonstrates that upon adoptive BM transplantation, genetically-modified hematopoietic cells differentiate into CNS microglia in a site-selective manner. The immediate precursors of these microglia most likely are mature BM mononuclear cells, which have been shown to enter the brain and engraft after transplantation into lethally irradiated mice[11]. Microglial engraftment was specifically enhanced by neuropathology, suggesting that myeloid cells may be used as vehicles for gene delivery to the CNS. It is conceivable that BM stem cells sense injury to the nervous system, mobilize into the blood and undergo microglial differentiation at the sites of CNS damage. In fact, hematopoietic stem cells have hepatic reconstitution activity[12], and GFP-marked primitive BM cells were recently found to regenerate infarcted myocardium[13].

The decreased propensity of the MSCV promoter to transcriptional silencing *in vivo* is of particular relevance in the CNS where gene silencing is pertinent. In fact, Krall *et al.* have observed that increases in BM-derived cells in the CNS predicted by PCR (10-fold) at 3–4 months post-BM transplant were not mirrored by similar increases in cells expressing the marker gene product (2-fold)[14]. Due to its high sensitivity, GFP is a useful marker for tracking hematopoietic cell progeny in the brain[5], and earlier studies addressing microglial turnover may have suffered from the fact that microglia either did not express readily detectable levels of antigen, or that additional *in situ* hybridization techniques were required to identify BM-derived cells[2,15,16]. GFP is generally believed to be biologically inert[17], and mice transplanted with GFP-expressing hematopoietic cells engrafted with normal kinetics and displayed normal blood counts. Although we cannot exclude the possibility that whole body irradiation promoted the engraftment of BM-derived cells in the CNS, the radiation dose used in our study was standard[2,3,14–16,18]. Irradiation and injection of congenic BM does not affect the phenotype of leukocytes in the brain[19]. Moreover, [^{3}H]thymidine-labeled monocytes find their way into the brain despite an intact blood–brain barrier[20], and recent experimental evidence in BM chimeras suggests that the number of cells that engraft in the CNS is the same, irrespective of whether the animals were irradiated or not[2,4]. It should also be noted that total body irradiation at 12 Gy applied in four split doses is currently used in the conditioning regimen for hematopoietic stem-cell transplantation in patients with multiple sclerosis[21].

A remarkable feature of CNS microglial engraftment is the propensity of gene-modified hematogenous cells to be attracted to sites of neuronal injury. Thus, BM-derived cells were found to differentiate into microglia in the ischemic hemisphere following stroke. Moreover, gene-marked microglia were detected in the deafferented lateral septum after ff-t, which parallels the physiological microglial activation observed with this lesion paradigm[10]. The data support recent results suggesting microglial engraftment and therapeutic benefit in murine models of rare metabolic disorders, such as globoid cell leukodystrophy and Sandhoff disease[22,23]. Even after remote lesion of the CNS, BM-derived microglia covered the somata of injured facial motoneurons during retrograde reaction. This site-specific influx of BM-derived cells despite an intact blood–brain barrier suggests that neurons may signal damage to circulating cells via specific molecular mediators, such as monocyte chemoattractant protein-1 (ref. 24). The

Methods

Retroviral transduction and BM transplantation. Gene transfer into hematopoietic cells was performed as described[5]. Briefly, BM cells from 8–12-week-old male C57BL/6 mice treated with 5-fluoruracil were stimulated with 20 ng/ml IL-3, 50 ng/ml IL-6 (PromoCell, Heidelberg. Germany) and 50 ng/ml SCF (provided by Amgen, Thousand Oaks, California) for 48 h. Subsequently, BM cells were co-cultured with irradiated (1,300 cGy) GP+E86 viral producer cells. After another 48 h, non-adherent BM cells were transplanted into lethally irradiated (two doses of 550 cGy 3 h apart) adult male C57BL/6 mice. BM cells from 8–12-week-old GFP-transgenic mice[7] were transplanted directly into irradiated wild-type mice. All recipient mice received 5×10^6 cells by tail vein injection.

Flow cytometry of GFP-expression in peripheral-blood cells. 4–15 weeks after BM transplant, peripheral-blood was examined by FACS (Becton Dickinson, Heidelberg, Germany). After erylysis, cells labeled with Mac-1-Pe, B220-Pe, Gr-1-Pe and CD4-Pe (Pharmingen, Heidelberg, Germany), were analyzed for GFP-expression. Dead cells (propidium iodide-positive) were excluded. Data were evaluated using the Cellquest software.

Analysis of donor cell engraftment in the CNS. After transcardial perfusion with 4% paraformaldehyde, 20 μm cryosections or 30–80 μm vibratome sections were obtained from the brains. Sections were incubated in PBS containing 5% normal goat serum. Primary and preabsorbed antibodies were added overnight at a dilution of 1:70 for Iba1 (ref. 8) (Imai, Japan), 1:50 for F4/80 (Serotec, Oxford, UK), 1:500 for GFP (Clontech, Palo Alto, California), 1:50 for MHC classI (BMA, Augst, Switzerland), 1:25 for MHC class II (Serotec) and 1:300 for choline acetyltransferase (Boehringer Mannheim, Mannheim, Germany). Texas Red- or Cy3-conjugated secondary antibodies (Molecular Probes, Leiden, The Netherlands; Dianova, Hamburg, Germany) were added at a dilution of 1:100 for 1 h. Incubation with biotinylated secondary antibody (1:100; Vector, Burlingame, California) was followed by avidin-biotin-peroxidase complex (ABC; Vector) and 3,3′-diaminobenzidine/H_2O_2 (Sigma, Deisenhofen, Germany) according to the manufacturers' instructions. The TUNEL-assay was performed using a commercially available kit and rhodamine-conjugated anti-digoxigenin antibody (Intergen, Heidelberg, Germany). The specificity of all stainings was controlled by omission of primary antibodies or terminal deoxynucleotidyl-transferase, resulting in no visible immunoreactivity. Acetylcholinesterase histochemistry was performed according to a modified Karnovsky-Roots protocol[10]. Nuclei were counterstained using Hoechst (Calbiochem, Bad Soden, Germany). For electron microscopy, immunostained sections were fixed in 2% glutaraldehyde/PBS, immersed in 2% Dalton's osmium and embedded in araldite. 1 μm semi-thin araldite sections were scanned for GFP-immunoreactivity, and adjacent ultrathin sections were mounted on mesh copper grids and processed for electron microscopy.

Quantification of regional microglial engraftment. 4 independent investigators counted the GFP-expressing ramified cells among up to 5,000 randomly selected Iba1$^+$ or F4/80$^+$ macrophages/microglia per animal (n = 15). Engraftment following injury was quantified by counting all GFP-expressing cells in lesioned and control brain areas of 2–3 representative sections per animal (n = 6).

Surgical procedures. 4 wk after BM transplant, ischemia was induced in mice (n = 8) by filament occlusion of the MCA (ref. 25), and verified by laser Doppler flowmetry. After 60 min, the monofilament was withdrawn to reperfuse the brain. Animals were killed after 1–14 d. Uni- and bilateral ff-t was induced in BM chimeras (n = 11) 10 wk post-transplantation. The fimbria-fornix was transected under visual guidance by aspiration[10]. Complete ff-t was verified by loss of hippocampal acetylcholinesterase staining. Unilateral facial nerve axotomy was induced in BM chimeras (n = 9) 14 wk post-transplantation by transection of the facial nerve at the stylomastoid foramen, resulting in ipsilateral whisker paresis. Animals were killed after 7–28 d.

spatiotemporal kinetics of microglial engraftment following BM transplant are unlikely to be explained by these mechanisms, given that the number of BM-derived microglia increased in some regions of the brain and decreased in others in the absence of obvious pathological changes or increased host-cell apoptosis. Thus, the factors governing 'physiological' microglial engraftment may be distinct from those operative under pathophysiological conditions.

In conclusion, our results suggest that BM transplantation might lead to significant microglial engraftment in the human CNS. Importantly, microglial engraftment is enhanced in the case of brain damage, suggesting that gene-modified hematopoietic cells provide a novel noninvasive approach to target potential therapeutic factors to the diseased CNS.

Acknowledgments: We thank P. Grämmel, D. Büringer, K. Brückner, S. Bauer and A. Sittler for their assistance. The work was partly supported by DFG and the Schilling foundation.

1. Kreutzberg, G.W. Microglia: a sensor for pathological events in the CNS. *Trends Neurosci.* **19**, 312–318 (1996).
2. Eglitis, M.A. & Mezey, É. Hematopoietic cells differentiate into both microglia and macroglia in the brains of adult mice. *Proc. Natl. Acad. Sci. USA* **94**, 4080–4085 (1997).
3. Brazelton, T.R., Rossi, F.M.V., Keshet, G.I. & Blau, H.M. From marrow to brain: expression of neuronal phenotypes in adult mice. *Science* **290**, 1775–1779 (2000).
4. Mezey, É, Chandross, K.J., Harta, G., Maki, R.A. & McKercher, S.R. Turning blood into brain: cells bearing neuronal antigens generated in vivo from bone marrow. *Science* **290**, 1779–1782 (2000).
5. Persons, D.A. *et al.* Retroviral-mediated transfer of the green fluorescent protein gene into murine hematopoietic cells facilitates scoring and selection of transduced progenitors in vitro and identification of genetically modified cells in vivo. *Blood* **90**, 1777–1786 (1997).
6. Pawliuk, R., Eaves, C. & Humphries, R. Sustained high-level reconstitution of the hematopoietic system by preselected hematopoietic cells expressing a transduced cell-surface antigen. *Hum. Gene Ther.* **8**, 1595–1604 (1997).
7. Okabe, M., Ikawa, M., Kominami, K., Nakanishi, T. & Nishimune, Y. Green mice as a source of ubiquitous green cells. *FEBS Lett.* **407**, 313–319 (1997).
8. Imai, Y. *et al.* A novel gene *Iba1* in the major histocompatibility complex class III region encoding an EF hand protein expressed in a monocytic lineage. *Biochem. Biophys. Res. Commun.* **224**, 855–862 (1996).
9. Carson, M.J., Reilly, C.R., Sutcliffe, J.G. & Lo, D. Mature microglia resemble immature antigen-presenting cells *Glia* **22**, 72–85 (1998).
10. Hollerbach, E.H., Haas, C.A., Hildebrandt, H., Frotscher, M. & Naumann, T. Region-specific activation of microglial cells in the rat septal complex following

fimbria-fornix transection. *J. Comp. Neurol.* **390**, 481–496 (1998).
11. Kennedy, D.W. & Abkowitz, J.L. Mature monocytic cells enter tissues and engraft. *Proc. Natl. Acad. Sci. USA* **95**, 14944–14949 (1998).
12. Lagasse, E. *et al.* Purified hematopoietic stem cells can differentiate into hepatocytes *in vivo*. *Nature Med.* **6**, 1229–1234 (2000).
13. Orlic, D. *et al.* Bone marrow cells regenerate infarcted myocardium. *Nature* **410**, 701–705 (2001).
14. Krall, W.J. *et al.* Cells expressing human glucocerebrosidase from a retroviral vector repopulate macrophages and central nervous system microglia after murine bone marrow transplantation. *Blood* **83**, 2737–2748 (1994).
15. Hickey, W.F. & Kimura, H. Perivascular microglial cells of the CNS are bone marrow-derived and present antigen in vivo. *Science* **239**, 290–292 (1988).
16. Hickey, W.F., Vass, K. & Lassmann, H. Bone marrow-derived elements in the central nervous system: an immunohistochemical and ultrastructural survey of rat chimeras. *J. Neuropathol. Exp. Neurol.* **51**, 246–256 (1992).
17. Goldman, S. & Roy, N. Human neural progenitor cells: better blue than green? *Nature Med.* **6**, 483–484 (2000).
18. Kennedy, D.W. & Abkowitz, J.L. Kinetics of central nervous system microglial and macrophage engraftment: Analysis using a transgenic bone marrow transplantation model. *Blood* **90**, 986–993 (1997).
19. Schlüter, D. *et al.* Regulation of microglia by $CD4^+$ and $CD8^+$ T cells: selective analysis in CD45-congenic normal and *Toxoplasma gondii*-infected bone marrow chimeras. *Brain Pathol.* **11**, 44–55 (2001).
20. Lawson, L.J., Perry, V.H. & Gordon, S. Turnover of resident microglia in the normal adult mouse brain. *Neuroscience* **48**, 405–415 (1992).
21. Burt, R.K. *et al.* Gene-marked autologous hematopoietic stem cell transplantation of autoimmune disease. *J. Clin. Immunol.* **20**, 1–9 (2000).
22. Wu, Y.-P. *et al.* Distribution and characterization of GFP^+ donor hematogenous cells in twitcher mice after bone marrow transplantation. *Am. J. Pathol.* **156**, 1849–1854 (2000).
23. Wada, R., Tifft, C.J. & Proia, R.L. Microglial activation precedes acute neurodegeneration in Sandhoff disease and is suppressed by bone marrow transplantation. *Proc. Natl. Acad. Sci. USA* **97**, 10954–10959 (2000).
24. Flügel, A. *et al.* Neuronal MCP-1 expression in response to remote nerve injury. *J. Cereb. Blood Flow Metab.* **21**, 60–76 (2001).
25. Hara, H., Huang, P.L., Panahian, N., Fishman, M.C. & Moskowitz, M.A. Reduced brain edema and infraction in mice lacking the neuronal isoform of nitric oxide synthase after transient MCA occlusion. *J. Cereb. Blood Flow Metab.* **16**, 605–611 (1996).

ON THE MARKET

ASSORTED ASSAYS

Mouse interferon-alpha ELISA.

PBL Biomedical Laboratories offers an **ELISA kit for measuring mouse interferon alpha** (Mu-IFN-α). The kit detects Mu-IFN- αA, α1, α4, α5, α6 and α9 in serum or media using a sandwich immunoassay. It is said to show no cross-sensitivity with mouse IFN-β, mouse IFN-γ or human IFN-α. The kit includes all the required reagents, as well as a pre-coated, 96-well microtiter breakaway strip plate.

Tel. (+1) 732-828-8881
Fax (+1) 732-828-3736
www.pblbio.com

BioLISA **kits for human TNF-α and VEGF-A** are now available from Bender MedSystems. The company says that the BioLISA technique achieves high specificity by binding the natural receptor, rather than an antibody, to the microtiter plate. As a result, it says that only the targeted bioactive cytokine is detected. Typical applications for the human TNF-α and the human VEGF-A BioLISAs are the detection and measurement of active tumor necrosis factor alpha and VEGF-A, respectively. These assays can be used with biological samples such as cell-culture supernatants, human serum and plasma.

Tel. (+43) 1-796-40-40-0
Fax (+43) 1-796-40-40-400
www.bendermedsystems.com

IMPROVING YOUR IMAGE

Bio-Rad Microscience has come up with a **laser-scanning microscope system** that is designed to be upgraded as research methodologies advance. The system specification for the Radiance2100 can be progressively upgraded from single-channel confocal through to multi-channel, multi-photon systems—as required. For example, researchers could start with a single-channel system with a 4-line Argon laser and upgrade it by adding further detectors and lasers such as HeCd, green HeNe and red diode lasers. The company's wide choice of laser line options, including the new 405 nm blue diode laser, offers alternatives across the range to suit a wide range of application needs. Radiance2100 is compatible with a range of upright and inverted microscopes from Nikon, Zeiss and Olympus.

Tel. (+44) (0) 20-8328-2111
Fax (+44) (0) 20-8328-2500

GENE EXPRESSION STUDIES

Tissue **microarrays for high-throughput screening of in situ gene expression for target validation** are now available from InnoGenex. The arrays are available from diseased and normal tissues, mouse normal tissues and rat normal tissues. These histologically characterized slides are said to be useful for molecular biologists and other researchers to understand the correlation of the gene and protein expression profile in normal and diseased tissues. They are suitable for the rapid screening of *in situ* differential expression of genes, identifying novel antibody markers, animal model studies, or for any other application that would use traditional tissue sections. Low-density arrays contain 20 to 50 elements per slide; high-density arrays have 100–200. All the donor tissue blocks and the final tissue arrays are validated for use in immunohistochemistry and *in situ* hybridization assays.

Tel. (+1) 925-543-1400
Fax (+1) 925-543-1405
www.innogenex.com

DETECTION SYSTEMS

Beckman Coulter: exclusive distributor of KineticScan HCS reader.

Beckman Coulter is now the exclusive distributor of the new KineticScan HCS Reader from Cellomics. The integration of this new detector on the Sagian Core System extends the application of these systems into high-content, cell-based screening for improved compound lead optimization. Whereas some readers deliver one piece of information from each assay well, the new **reader for cell-based assays** analyzes the response of live cells, generating multiple images and parameter data for each microplate well. Beckman Coulter will also market Cellomics' Hitkits HCS reagent kits for more than 20 assays, including cell motility, multiparameter apoptosis and cell viability.

Tel. (+1) 714-871-4848
Fax (+1) 714-773-6611
www.beckmancoulter.com